

BRIEF REPORT



Design, synthesis, biological evaluation and molecular docking study of 2,4-diarylimidazoles and 2,4-bis(benzyloxy)-5-arylpyrimidines as novel HSP90 N-terminal inhibitors

Man Yang, Chenyao Li, Yajing Li, Chen Cheng, Meiyun Shi, Lei Yin, Hongyu Xue and Yajun Liu 

School of Life and Pharmaceutical Sciences, Dalian University of Technology, Panjin, China

ABSTRACT

The molecular chaperone HSP90 plays an essential role in cancer occurrence and development. Therefore, it is an important target for the development of anticancer drugs. 1,3-Dibenzyl-2-aryl imidazolidine (**8**) is a previously reported inhibitor of HSP90; however, its anticancer activity is poor. In this work, chemical modification of **8** led to the discovery of 2,4-diarylimidazoles and 2,4-bis(benzyloxy)-5-arylpyrimidines as two types of novel HSP90 N-terminal inhibitors. **16l** and **22k** exhibited antiproliferative activity against multiple breast cancer cell lines with IC₅₀ values at the low micromolar level. **16l** and **22k** induced significant degradation of the client proteins AKT and ERK and a lower level of the heat shock response in comparison with tanespimycin (17-AAG). **22k** exhibited a strong affinity for the HSP90 α N-terminus with an IC₅₀ value of 0.21 μ M. A molecular docking study revealed that **16l** and **22k** successfully bind to the geldanamycin binding site at the N-terminus of HSP90 α .

ARTICLE HISTORY

Received 24 June 2022
Revised 8 September 2022
Accepted 9 September 2022

KEYWORDS

HSP90; 2,4-diarylimidazoles; 2,4-bis(benzyloxy)-5-arylpyrimidines; molecular docking; anticancer

Introduction



Because proteins play roles in nearly every cellular process, it is essential to maintain protein homeostasis to preserve normal cell functions. Molecular chaperones are a large family of proteins that guard cellular protein homeostasis by regulating the conformation and quality of client proteins^{1,2}. Heat shock protein 90 (HSP90) is one of the most crucial molecular chaperones in eukaryotes and stabilises and activates more than 400 client proteins^{3,4}. Because cancer cells require higher levels of proteins for survival than normal cells, HSP90 is overexpressed in cancer cells, accounting for 4–6% of the whole proteome^{5,6}. In addition, conformations of normal HSP90 and HSP90 of the cancer phenotype are different, and the latter is more susceptible to inhibitors⁷. Inhibition of HSP90 in cancer cells results in the degradation of client oncoproteins via the ubiquitin-proteasome pathway and the subsequent disruption of multiple signal transduction pathways, further leading to the apoptosis of cancer cells^{8,9}. Therefore, HSP90 is a promising therapeutic target for discovering anticancer drugs¹⁰. Beyond cancer, HSP90 has also emerged as a potential drug target in other protein-related diseases, such as neurodegenerative diseases, infectious diseases, and ageing^{11–14}.


HSP90 consists of three domains: the N-terminus, C-terminus, and the middle domain^{15,16}. Classical HSP90 inhibitors competitively bind to the ATP binding pocket at the N-terminus. Over twenty HSP90 N-terminal inhibitors have entered clinical trials for the treatment of a variety of cancers^{17,18}. Allosteric binding sites are also found at the C-terminus and the middle domain. HSP90 C-terminal inhibitors have been extensively studied in recent years because they do not cause a rescue cascade known as the heat shock response, which is often observed in the modulation of

HSP90 with N-terminal inhibitors^{19,20}. Many natural products and synthetic small molecules have been identified as HSP90 C-terminal inhibitors; however, they have not yet entered clinical trials for cancer therapy²¹.

Although some clinical investigations of HSP90 N-terminal inhibitors have stopped or terminated because of drug resistance and/or organ toxicity, there are still a considerable number of active inhibitors in clinical trials^{22,23}. According to the results obtained from ClinicalTrials.gov (<https://www.clinicaltrials.gov/>, 2022/06/17), 17 studies are ongoing or in preparation (including recruiting, enrolling by invitation, and active/not recruiting). Some representative examples (1–7) currently being evaluated in clinical trials are shown in Figure 1. It should be noted that combination therapy of HSP90 N-terminal inhibitors with other anticancer drugs represents an effective strategy to combat cancer in clinical trials at present²⁴. Combination with HSP90 inhibitors would help to prevent the chemotherapeutic resistance of classical anticancer drugs and/or potentiate the cytotoxic effects^{25,26}. In this context, it is still desirable to develop more HSP90 N-terminal inhibitors as novel anticancer agents.

We previously reported that a series of 1,3-dibenzyl-2-aryl imidazolidines **8** served as HSP90 N-terminal inhibitors²⁷ (Figure 2). These inhibitors showed a strong affinity for the HSP90 N-terminus according to the fluorescence polarisation (FP) assay; however, they exhibited weak antiproliferative activity against cancer cells such as MCF-7 and A549. Weak anticancer efficacy may be attributed to the physicochemical instability of the imidazolidine ring because **8** is converted into the corresponding benzaldehyde and *N,N'*-dibenzyl ethylenediamine in an aqueous medium^{28–30}. Therefore, we hypothesised that replacing imidazolidine with

CONTACT Yajun Liu  yjliu85@dlut.edu.cn  School of Life and Pharmaceutical Sciences, Dalian University of Technology, Panjin, China

 Supplemental data for this article can be accessed online at <https://doi.org/10.1080/14756366.2022.2124407>.

© 2022 The Author(s). Published by Informa UK Limited, trading as Taylor & Francis Group.

This is an Open Access article distributed under the terms of the Creative Commons Attribution License (<http://creativecommons.org/licenses/by/4.0/>), which permits unrestricted use, distribution, and reproduction in any medium, provided the original work is properly cited.

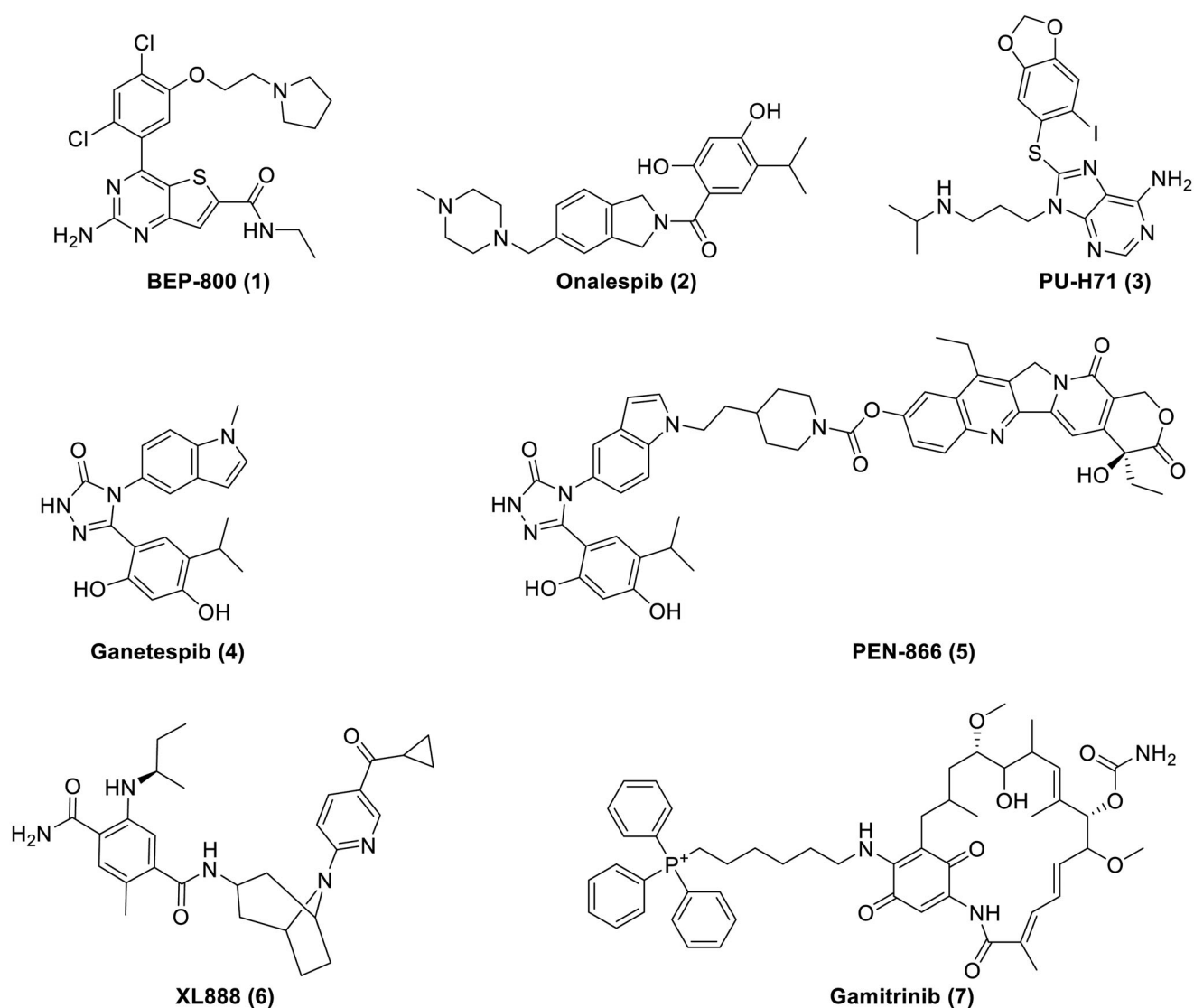


Figure 1. Representative HSP90 N-terminal inhibitors in clinical trials.

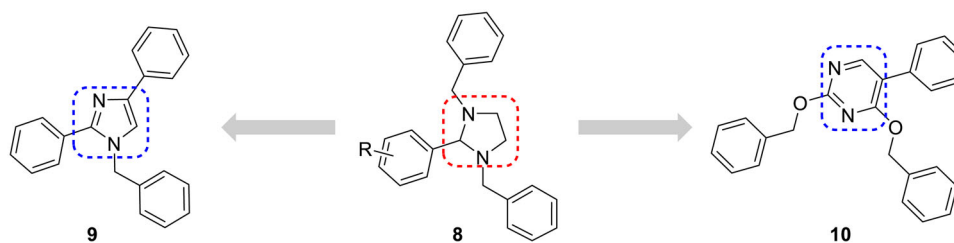


Figure 2. Design strategy illustration.

stable aromatic scaffolds would lead to the discovery of novel HSP90 N-terminal inhibitors with stronger anticancer activity. Therefore, the nonaromatic imidazolidine ring was replaced by the aromatic imidazole ring and pyrimidine ring, which are frequently used in clinical drugs^{31,32}. As shown in **Figure 2**, trisubstituted imidazole **9** and pyrimidine **10** were designed to develop novel HSP90 inhibitors. Compound **9** bears a benzyl group at the N1 position and two phenyl groups at the C2 and C4 positions of the imidazole ring. In the case of **10**, it has two benzyloxy groups at the C2 and C4 positions and a phenyl group at the C5 position of the pyrimidine ring.

Materials and methods

Chemistry

General method for chemistry

All chemical reagents were commercially purchased and used without further purification. Reactions were monitored by thin layer chromatography on GF254 TLC plates. Column chromatography purification was performed on silica gel (200–300 mesh). Nuclear magnetic resonance (NMR) data were collected on an AVANCE III HD 500 MHz nuclear magnetic resonance spectrometer (Bruker, Billerica, MA, USA). HRMS detection of **16** and **22** were

carried out on a Q Exactive mass spectrometer (Thermo Fisher, Waltham, MA USA) with electrospray ionisation (ESI) as the ionisation source. Mass spectra of **19** and **20** were recorded by a UPLC–ESI–MS/MS system. The UPLC–ESI–MS/MS system consists of an Acquity UPLC system (Waters Corp., MA, USA) coupled with a QTRAP 6500 Plus mass spectrometer (Sciex, Toronto, Canada) equipped with a TurbolonSpray source. Analyst Software 1.6.3 was used for data acquisition and data processing.

Preparation of 1-benzyl-4-bromo-1H-imidazoles (**13**)

13 was synthesised using a modified reported method³³. To a solution of 4-bromo-1H-imidazole (**11**, 8.00 g, 54.40 mmol) in acetone (70 ml), benzyl bromide (**12**, 7.20 ml, 60.40 mmol) and potassium carbonate (8.28 g, 60.00 mmol) were added. The reaction mixture was stirred at room temperature for 22 h. Potassium carbonate was filtered, and acetone was removed under a vacuum. Water and ethyl acetate were added to extract the product. The organic layer was collected, washed with water and brine, dried over anhydrous magnesium sulphate, and condensed under a vacuum. The resulting crude product was dissolved in a small amount of dichloromethane and then precipitated by the addition of petroleum ether. The solid was filtered to afford **13** as a white solid (5.71 g, 44.07%).

General synthetic procedure for 1-benzyl-4-aryl-1H-imidazoles (**14**)

14 was synthesised using a modified procedure³⁴. To a solution of 1-benzyl-4-bromo-1H-imidazoles (**13**, 2.38 g, 10 mmol) in 1,4-dioxane (18 ml), aryl boronic acid (2.5 equiv.), Pd(dppf)Cl₂ (5 mol%) and aqueous Na₂CO₃ solution (2.12 g in 6 ml water, 20 mmol) were added. The reaction mixture was heated to reflux and stirred under a nitrogen atmosphere for 4 h. After cooling to room temperature, the reaction mixture was extracted with water and ethyl acetate. The organic layer was collected, washed with water and brine, dried over anhydrous magnesium sulphate, and condensed under a vacuum. The resulting crude product was purified by column chromatography using petroleum ether/ethyl acetate as the eluent.

General synthetic procedure for 1-benzyl-2-bromo-4-aryl-1H-imidazoles (**15**)

15 was prepared using a modified reported method³⁵. To a solution of 1-benzyl-4-aryl-1H-imidazoles (**14**) in CCl₄ (2.0 M), *N*-bromosuccinimide (NBS, 2 equiv.) was added. The reaction mixture was stirred at 35 °C for 14 h. The reaction mixture was extracted with dichloromethane and water. The organic layer was collected, washed with water and brine, dried over anhydrous magnesium sulphate, and condensed under a vacuum. The resulting crude product was purified by column chromatography using petroleum ether/ethyl acetate as the eluent.

General synthetic procedure for 1-benzyl-2,4-diaryl-1H-imidazoles (**16**)

16 was prepared using a procedure similar to that for **14**. To a solution of 1-benzyl-2-bromo-4-aryl-1H-imidazoles (**15**) in 1,4-dioxane, aryl boronic acid (2.5 equiv.), Pd(dppf)Cl₂ (5 mol%) and aqueous Na₂CO₃ solution (3.3 M, 2.5 equiv.) was added. The reaction mixture was heated to reflux and stirred under a nitrogen atmosphere for 4 h. After cooling to room temperature, the reaction mixture was extracted with water and ethyl acetate. The organic layer was collected, washed with water and brine, dried

over anhydrous magnesium sulphate, and condensed under a vacuum. The resulting crude product was purified by column chromatography using petroleum ether/ethyl acetate as the eluent.

1-Benzyl-2,4-diphenyl-1H-imidazole (16a). White solid, yield 29.13%. ¹H NMR (500 MHz, Chloroform-*d*) δ 7.65 (s, 1H), 7.51–7.49 (m, 2H), 7.43–7.35 (m, 3H), 7.28–7.18 (m, 7H), 7.14–7.11 (m, 1H), 6.97 (d, *J* = 7.0 Hz, 2H), 4.97 (s, 2H). ¹³C NMR (126 MHz, Chloroform-*d*) δ 138.32, 137.12, 136.59, 134.54, 130.96, 130.56, 128.92, 128.82, 128.79, 128.71, 128.12, 127.91, 126.93, 126.52, 126.33, 48.77. HRMS (ESI, *m/z*) calcd for C₂₂H₁₉N₂ [M + H]⁺ 311.1548, found 311.1560.

1-Benzyl-4-phenyl-2-(*m*-tolyl)-1H-imidazole (16b). White solid, yield 35.28%. ¹H NMR (500 MHz, Chloroform-*d*) δ 7.64 (d, *J* = 3.0 Hz, 1H), 7.54–7.49 (m, 2H), 7.28–7.25 (m, 4H), 7.23–7.17 (m, 3H), 7.23–7.10 (m, 4H), 7.03 (d, *J* = 8.0 Hz, 1H), 6.98 (s, 3H), 4.94 (s, 2H), 2.29 (s, 3H). ¹³C NMR (126 MHz, Chloroform-*d*) δ 138.57, 137.97, 136.95, 136.62, 134.48, 131.58, 130.35, 129.51, 129.03, 128.76, 128.12, 127.90, 127.05, 126.45, 126.31, 48.85, 21.33. HRMS (ESI, *m/z*) calcd for C₂₃H₂₁N₂ [M + H]⁺ 325.1705, found 325.1715.

1-Benzyl-2-(3-chlorophenyl)-4-phenyl-1H-imidazole (16c). White solid, yield 32.46%. ¹H NMR (500 MHz, Chloroform-*d*) δ 7.68 (s, 1H), 7.49–7.45 (m, 2H), 7.38–7.36 (m, 1H), 7.36–7.25 (m, 4H), 7.25–7.19 (m, 2H), 7.17–7.16 (m, 2H), 7.09–7.06 (m, 1H), 6.98–6.95 (m, 2H), 4.97 (s, 2H). ¹³C NMR (126 MHz, Chloroform-*d*) δ 138.90, 137.46, 136.14, 134.68, 133.97, 132.34, 130.88, 130.15, 129.28, 128.95, 128.89, 128.24, 128.12, 127.28, 126.96, 126.70, 49.09. HRMS (ESI, *m/z*) calcd for C₂₂H₁₈ClN₂ [M + H]⁺ 345.1159; found 345.1172.

1-Benzyl-4-phenyl-2-(*p*-tolyl)-1H-imidazole (16d). White solid, yield 41.00%. ¹H NMR (500 MHz, Chloroform-*d*) δ 7.62 (s, 1H), 7.51 (d, *J* = 7.5 Hz, 2H), 7.29–7.25 (m, 3H), 7.22–7.09 (m, 7H), 7.02–6.97 (m, 2H), 4.95 (s, 2H), 2.40 (s, 3H). ¹³C NMR (126 MHz, Chloroform-*d*) δ 138.61, 138.10, 136.98, 136.74, 134.67, 130.79, 129.67, 128.91, 128.78, 128.10, 127.86, 127.42, 126.91, 126.46, 126.24, 48.63, 21.38. HRMS (ESI, *m/z*) calcd for C₂₃H₂₁N₂ [M + H]⁺ 325.1705, found 325.1714.

1-(4-(1-Benzyl-4-phenyl-1H-imidazol-2-yl)phenyl)ethan-1-one (16e). White solid, yield 64.45%. ¹H NMR (500 MHz, Chloroform-*d*) δ 7.97–7.91 (m, 2H), 7.69 (s, 1H), 7.48–7.43 (m, 2H), 7.33–7.26 (m, 5H), 7.24–7.15 (m, 3H), 7.00–6.93 (m, 2H), 5.01 (s, 2H), 2.62 (s, 3H). ¹³C NMR (126 MHz, Chloroform-*d*) δ 197.56, 139.35, 137.92, 136.88, 136.26, 135.51, 134.10, 131.06, 128.92, 128.80, 128.27, 128.10, 127.57, 126.84, 126.76, 48.99, 26.68. HRMS (ESI, *m/z*) calcd for C₂₄H₂₁N₂O [M + H]⁺ 353.1654, found 353.1661.

1-Benzyl-2-(4-chlorophenyl)-4-phenyl-1H-imidazole (16f). White solid, yield 34.40%. ¹H NMR (500 MHz, Chloroform-*d*) δ 7.67 (s, 1H), 7.50–7.45 (m, 2H), 7.35–7.32 (m, 2H), 7.29–7.26 (m, 3H), 7.22–7.20 (m, 2H), 7.17–7.11 (m, 3H), 6.97–6.95 (m, 2H), 4.97 (s, 2H). ¹³C NMR (126 MHz, Chloroform-*d*) δ 138.86, 137.50, 136.38, 134.85, 134.22, 132.26, 129.23, 129.02, 128.88, 128.23, 128.03, 127.42, 126.77, 126.59, 48.84. HRMS (ESI, *m/z*) calcd for C₂₂H₁₈ClN₂ [M + H]⁺ 345.1159, found 345.1171.

4-(1-Benzyl-4-phenyl-1H-imidazol-2-yl)phenol (16g). White solid, yield 37.00%. ¹H NMR (500 MHz, DMSO-*d*₆) δ 9.73 (s, 1H), 7.90 (s, 1H), 7.45–7.40 (m, 2H), 7.30–7.22 (m, 3H), 7.18 (t, *J* = 7.5 Hz, 2H), 7.09 (t, *J* = 7.3 Hz, 1H), 7.00 (d, *J* = 8.5 Hz, 2H), 6.93 (t, *J* = 7.5 Hz, 2H), 6.80 (t, *J* = 8.5 Hz, 2H), 5.02 (s, 2H). ¹³C NMR (126 MHz,

DMSO- d_6) δ 158.17, 138.01, 137.88, 137.13, 135.53, 132.45, 128.96, 128.47, 127.90, 127.27, 126.29, 126.14, 120.93, 116.30, 48.10. HRMS (ESI, m/z) calcd for $C_{22}H_{19}N_2O$ $[M + H]^+$ 327.1497, found 327.1493.

1-Benzyl-2-(furan-2-yl)-4-phenyl-1H-imidazole (16h). White solid, yield 19.07%. 1H NMR (500 MHz, Chloroform- d) δ 7.64 (s, 1H), 7.58 (d, $J=7.5$ Hz, 2H), 7.53 (d, $J=1.8$ Hz, 1H), 7.34–7.19 (m, 6H), 7.06 (d, $J=7.0$ Hz, 2H), 6.46–6.44 (m, 1H), 6.32 (d, $J=3.0$ Hz, 1H), 5.08 (s, 2H). ^{13}C NMR (126 MHz, Chloroform- d) δ 143.45, 143.24, 141.88, 138.10, 136.28, 134.07, 128.82, 128.24, 127.06, 127.04, 126.75, 118.85, 112.47, 111.29, 49.36. HRMS (ESI, m/z) calcd for $C_{20}H_{17}N_2O$ $[M + H]^+$ 301.1341, found 301.1349.

1-Benzyl-4-phenyl-2-(thiophen-2-yl)-1H-imidazole (16i). White solid, yield 16.80%. 1H NMR (500 MHz, Chloroform- d) δ 7.67 (s, 1H), 7.60–7.54 (m, 2H), 7.45 (dd, $J=5.0, 1.5$ Hz, 1H), 7.31–7.22 (m, 2H), 7.21–7.15 (m, 1H), 7.07 (dd, $J=5.0, 3.5$ Hz, 1H), 7.05–7.00 (m, 2H), 6.93 (dd, $J=3.5, 1.1$ Hz, 1H), 5.02 (s, 2H). ^{13}C NMR (126 MHz, DMSO- d_6) δ 136.10, 133.17, 131.78, 129.38, 125.75, 125.59, 124.10, 123.88, 123.45, 123.24, 122.87, 122.19, 122.02, 121.85, 116.09, 44.07. HRMS (ESI, m/z) calcd for $C_{20}H_{17}N_2S$ $[M + H]^+$ 317.1112, found 317.1123.

1-Benzyl-2-(4-chlorophenyl)-4-(p-tolyl)-1H-imidazole (16j). White solid, yield 47.54%. 1H NMR (500 MHz, Chloroform- d) δ 7.67 (s, 1H), 7.36–7.32 (m, 4H), 7.29–7.25 (m, 3H), 7.12 (d, $J=8.5$ Hz, 2H), 7.03 (d, $J=8.0$ Hz, 2H), 7.00–6.94 (m, 2H), 4.96 (s, 2H), 2.29 (s, 3H). ^{13}C NMR (126 MHz, Chloroform- d) δ 138.77, 137.34, 136.34, 136.32, 134.81, 132.29, 131.15, 129.22, 129.02, 128.98, 128.89, 128.05, 127.00, 126.82, 126.55, 48.90, 21.14. HRMS (ESI, m/z) calcd for $C_{23}H_{20}ClN_2$ $[M + H]^+$ 359.1315, found 359.1327.

1-Benzyl-2-(4-chlorophenyl)-4-(m-tolyl)-1H-imidazole (16k). White solid, yield 23.00%. 1H NMR (500 MHz, Chloroform- d) δ 7.66 (s, 1H), 7.48 (s, 1H), 7.36–7.26 (m, 5H), 7.15–7.03 (m, 4H), 7.00–6.93 (m, 3H), 4.96 (s, 2H), 2.28 (s, 3H). ^{13}C NMR (126 MHz, Chloroform- d) δ 138.95, 137.93, 137.44, 136.41, 134.82, 134.07, 132.29, 129.19, 129.08, 128.89, 128.04, 128.02, 127.47, 127.40, 126.78, 123.63, 48.86, 21.46. HRMS (ESI, m/z) calcd for $C_{23}H_{20}ClN_2$ $[M + H]^+$ 359.1315, found 359.1324.

1-Benzyl-2,4-bis(4-chlorophenyl)-1H-imidazole (16l). White solid, yield 13.37%. 1H NMR (500 MHz, Chloroform- d) δ 7.65 (s, 1H), 7.45–7.37 (m, 2H), 7.36–7.31 (m, 2H), 7.30–7.26 (m, 3H), 7.21–7.14 (m, 2H), 7.13–7.07 (m, 2H), 6.99–6.91 (m, 2H), 4.95 (s, 2H). ^{13}C NMR (126 MHz, Chloroform- d) δ 137.87, 137.62, 136.23, 135.13, 132.81, 132.30, 132.18, 129.40, 128.94, 128.70, 128.43, 128.13, 127.84, 127.69, 126.82, 48.92. HRMS (ESI, m/z) calcd for $C_{22}H_{16}Cl_2N_2$ $[M + H]^+$ 379.0769, found 379.0783.

1-Benzyl-4-(3-chlorophenyl)-2-(4-chlorophenyl)-1H-imidazole (16m). White solid, yield 56.18%. 1H NMR (500 MHz, Chloroform- d) δ 7.67 (s, 1H), 7.58–7.57 (m, 1H), 7.37–7.34 (m, 2H), 7.30–7.26 (m, 3H), 7.22–7.20 (m, 1H), 7.13–7.10 (m, 4H), 6.96–6.93 (m, 2H), 4.96 (s, 2H). ^{13}C NMR (126 MHz, Chloroform- d) δ 137.62, 137.51, 136.09, 136.00, 135.20, 134.27, 132.13, 129.40, 129.37, 128.93, 128.43, 128.14, 128.09, 126.79, 126.69, 126.60, 124.50, 48.93. HRMS (ESI, m/z) calcd for $C_{22}H_{17}Cl_2N_2$ $[M + H]^+$ 379.0769, found 379.0786.

1-Benzyl-2-phenyl-4-(p-tolyl)-1H-imidazole (16n). White solid, yield 28.10%. 1H NMR (500 MHz, Chloroform- d) δ 7.64 (s, 1H), 7.38–7.35

(m, 5H), 7.30–7.26 (m, 3H), 7.25–7.18 (m, 2H), 7.01 (d, $J=8.0$ Hz, 2H), 6.98–6.94 (m, 2H), 4.96 (s, 2H), 2.27 (s, 3H). ^{13}C NMR (126 MHz, Chloroform- d) δ 138.20, 136.93, 136.50, 136.05, 131.41, 130.99, 130.52, 128.89, 128.79, 128.68, 128.40, 127.93, 126.98, 126.50, 48.84, 21.13. HRMS (ESI, m/z) calcd for $C_{23}H_{21}N_2$ $[M + H]^+$ 325.1705, found 325.1711.

1-Benzyl-4-phenyl-2-(thiophen-2-yl)-1H-imidazole (16o). White solid, yield 35.22%. 1H NMR (500 MHz, Chloroform- d) δ 7.60 (s, 1H), 7.45–7.40 (m, 3H), 7.27–7.25 (m, 5H), 7.08 (d, $J=5.0$ Hz, 1H), 6.96–6.94 (m, 2H), 6.86–6.83 (m, 2H), 4.94 (s, 2H). ^{13}C NMR (126 MHz, Chloroform- d) δ 138.20, 137.00, 136.35, 134.15, 131.14, 129.63, 129.15, 128.95, 128.82, 128.01, 127.78, 127.17, 126.95, 123.32, 122.25, 48.92. HRMS (ESI, m/z) calcd for $C_{20}H_{17}N_2S$ $[M + H]^+$, 317.1112, found 317.1125.

1-Benzyl-4-(4-chlorophenyl)-2-phenyl-1H-imidazole (16p). White solid, yield 27.83%. 1H NMR (500 MHz, Chloroform- d) δ 7.67 (s, 1H), 7.43–7.33 (m, 5H), 7.29–7.27 (m, 3H), 7.22–7.12 (m, 4H), 6.99–6.93 (m, 2H), 4.96 (s, 2H). ^{13}C NMR (126 MHz, Chloroform- d) δ 137.16, 137.10, 136.24, 133.97, 132.76, 132.15, 130.84, 130.00, 129.22, 129.04, 128.97, 128.85, 128.27, 128.04, 128.00, 127.33, 126.98, 48.93. HRMS (ESI, m/z) calcd for $C_{22}H_{18}ClN_2$ $[M + H]^+$ 345.1159, found 345.1172.

Preparation of 2,4-bis(4-chlorophenyl)-1H-imidazole (19)

19 was prepared using a modified procedure previously reported by the Li group³⁶. A mixture of 4-chlorobenzene-1-carboximide hydrochloride (2.61 g, 20 mmol), THF (36 ml) and H_2O (9 ml) was stirred and heated to 70 °C. α -Bromo-4-chloroacetophenone (4.20 g, 18 mmol) in THF (11 ml) was slowly added, and the reaction mixture was then stirred at 70 °C for 8 h. THF was removed under vacuum. The resulting mixture was dissolved in water and dichloromethane (30 ml/30 ml), and the slow addition of concentrated HCl led to the precipitation of the product, which was further filtered and washed with dichloromethane to afford **19** as a light yellow solid (1.12 g, 21.6%).

1H NMR (500 MHz, DMSO- d_6) δ 12.81 (s, 1H), 8.07–7.99 (m, 2H), 7.91–7.85 (m, 2H), 7.82 (s, 1H), 7.58–7.52 (m, 2H), 7.47–7.42 (m, 2H). ^{13}C NMR (126 MHz, DMSO- d_6) δ 144.89, 140.00, 133.33, 132.64, 130.45, 129.18, 128.75, 128.39, 126.51, 125.94, 115.15. LC-MS (ESI, m/z) 288.8 $[M + H]^+$.

General synthetic procedure for 1-substituted 2,4-bis(4-chlorophenyl)-1H-imidazoles (20)

Excess aliphatic halide and K_2CO_3 were added to a solution of 2,4-bis(4-chlorophenyl)-1H-imidazole (**19**) in the indicated solvent. The reaction mixture was stirred at the indicated temperature. The reaction mixture was extracted with ethyl acetate and water. The organic layer was collected, washed with water and brine, dried over anhydrous magnesium sulphate, and condensed under a vacuum. The resulting crude product was purified by column chromatography using petroleum ether/ethyl acetate as the eluent.

1-Allyl-2,4-bis(4-chlorophenyl)-1H-imidazole (20a). 20a was prepared from **19** (0.58 g, 2 mmol) and allyl bromide (6.92 ml, 20 mmol) in acetonitrile at 80 °C. White solid (79 mg, 11.9%). 1H NMR (500 MHz, chloroform- d) δ 7.76 (d, $J=8.0$ Hz, 2H), 7.59 (d, $J=8.0$ Hz, 2H), 7.44 (d, $J=8.0$ Hz, 2H), 7.34 (d, $J=8.0$ Hz, 2H), 7.27 (s, 1H), 6.03–6.01 (m, 1H), 5.35 (d, $J=10.5$ Hz, 1H), 5.19 (d, $J=17.0$ Hz, 1H), 4.61 (s, 2H). ^{13}C NMR (126 MHz, chloroform- d) δ

147.12, 140.43, 135.26, 132.97, 132.48, 132.40, 130.11, 128.91, 128.73, 126.17, 118.33, 117.06, 49.37, 29.71. LC-MS (ESI, m/z) 328.8 [M + H]⁺.

2,4-Bis(4-chlorophenyl)-1-pentyl-1H-imidazole (20b). 20b was prepared from 19 (0.29 g, 1 mmol) and 1-pentyl bromide (0.17 g, 1.1 mmol) in acetone at 60 °C. White solid (30 mg, 8.36%). ¹H NMR (500 MHz, chloroform-*d*) δ 7.75 (d, *J* = 8.0 Hz, 2H), 7.56 (d, *J* = 8.0 Hz, 2H), 7.45 (d, *J* = 8.0 Hz, 2H), 7.33 (d, *J* = 8.5 Hz, 2H), 7.28 (s, 1H), 3.96 (t, *J* = 7.5 Hz, 2H), 1.77 (t, *J* = 7.5 Hz, 2H), 1.30–1.25 (m, 4H), 0.87 (t, *J* = 7.0 Hz, 3H). ¹³C NMR (126 MHz, chloroform-*d*) δ 147.04, 140.20, 135.12, 132.37, 130.32, 128.93, 128.71, 126.11, 116.47, 47.08, 30.80, 28.62, 22.14, 13.84. LC-MS (ESI, m/z) 359.2 [M + H]⁺.

Methyl 2-(2,4-bis(4-chlorophenyl)-1H-imidazol-1-yl)acetate (20c). 20c was prepared from 19 (0.58 g, 2 mmol) and methyl bromoacetate (0.46 g, 3 mmol) in acetonitrile at 80 °C. White solid (420 mg, 58.2%). ¹H NMR (500 MHz, chloroform-*d*) δ 7.77–7.74 (m, 2H), 7.54–7.45 (m, 4H), 7.35–7.26 (m, 3H), 4.71 (s, 2H), 3.81 (s, 3H). ¹³C NMR (126 MHz, chloroform-*d*) δ 168.07, 147.72, 140.79, 135.63, 132.64, 132.16, 130.29, 129.12, 128.72, 128.17, 126.28, 117.62, 53.02, 48.22. LC-MS (ESI, m/z) 360.8 [M + H]⁺.

2-(2,4-Bis(4-chlorophenyl)-1H-imidazol-1-yl)acetamide (20d). 20d was prepared from 19 (0.58 g, 2 mmol) and bromoacetamide (0.414 g, 3 mmol) in DMF at 80 °C. White solid (120 mg, 17.3%). ¹H NMR (500 MHz, DMSO-*d*₆) δ 7.83–7.79 (m, 3H), 7.71 (s, 1H), 7.65 (d, *J* = 8.5 Hz, 2H), 7.57 (d, *J* = 8.5 Hz, 2H), 7.43 (d, *J* = 8.5 Hz, 2H), 7.39 (s, 1H), 4.71 (s, 2H). ¹³C NMR (126 MHz, DMSO-*d*₆) δ 168.52, 146.37, 138.18, 133.45, 133.02, 130.56, 129.92, 129.07, 128.55, 128.46, 125.79, 120.41, 49.05. LC-MS (ESI, m/z) 345.9 [M + H]⁺.

3-(2,4-Bis(4-chlorophenyl)-1H-imidazol-1-yl)propan-1-ol (20e). 20e was prepared from 19 (0.29 g, 1 mmol) and 3-bromo-1-propanol (132 μL, 1.1 mmol) in acetonitrile at 80 °C. White solid (143 mg, 41.2%). ¹H NMR (500 MHz, chloroform-*d*) δ 7.76–7.73 (m, 2H), 7.60–7.57 (m, 2H), 7.46–7.43 (m, 2H), 7.35–7.30 (m, 3H), 7.27 (s, 1H), 4.16 (t, *J* = 7.0 Hz, 2H), 3.62 (t, *J* = 5.5 Hz, 2H), 1.97 (t, *J* = 6.0 Hz, 2H). ¹³C NMR (126 MHz, chloroform-*d*) δ 147.12, 140.29, 135.25, 132.50, 132.35, 130.28, 129.00, 128.88, 128.76, 126.15, 116.84, 58.82, 43.68, 33.30. LC-MS (ESI, m/z) 347.3 [M + H]⁺.

General synthetic procedure for 2,4-bis(benzyloxy)-5-arylpyrimidines (22)

2,4-Bis(benzyloxy)-5-bromopyrimidine **21** is commercially available and was used without further purification. **22** was prepared using a procedure similar to that for **14**. To a solution of **21** in 1,4-dioxane (9 ml), aryl boronic acid (2.5 equiv.), Pd(dppf)Cl₂ (5 mol%) and aqueous Na₂CO₃ solution (3.3 M, 2.0 equiv.) was added. The reaction mixture was heated to reflux and stirred under a nitrogen atmosphere for 4 h. After cooling to room temperature, the reaction mixture was extracted with water and ethyl acetate. The organic layer was collected, washed with water and brine, dried over anhydrous magnesium sulphate, and condensed under a vacuum. The resulting crude product was purified by column chromatography using petroleum ether/ethyl acetate as the eluent.

2,4-Bis(benzyloxy)-5-phenylpyrimidine (22a). White solid, yield 38.55%. ¹H NMR (500 MHz, Chloroform-*d*) δ 8.31 (s, 1H), 7.53–7.50 (m, 4H), 7.44–7.27 (m, 11H), 5.50 (s, 2H), 5.46 (s, 2H). ¹³C NMR

(126 MHz, Chloroform-*d*) δ 167.45, 163.83, 158.11, 136.62, 136.23, 133.22, 128.81, 128.49, 128.47, 128.43, 128.08, 128.02, 127.95, 127.64, 127.54, 116.33, 69.23, 68.34. HRMS (ESI, m/z) calcd for C₂₄H₂₁N₂O₂ [M + H]⁺ 369.1603, found 369.1615.

2,4-Bis(benzyloxy)-5-(*o*-tolyl)pyrimidine (22b). White solid, yield 42.02%. ¹H NMR (500 MHz, Chloroform-*d*) δ 8.13 (s, 1H), 7.51 (d, *J* = 7.5 Hz, 2H), 7.39 (t, *J* = 8.0 Hz, 2H), 7.36–7.20 (m, 9H), 7.15 (d, *J* = 7.5 Hz, 1H), 5.46 (s, 2H), 5.45 (s, 2H), 2.14 (s, 3H). ¹³C NMR (126 MHz, Chloroform-*d*) δ 167.74, 164.14, 158.66, 137.33, 136.64, 136.26, 132.99, 130.41, 130.05, 128.50, 128.43, 128.20, 128.15, 128.06, 127.92, 127.60, 125.76, 116.56, 69.26, 68.13, 20.02. HRMS (ESI, m/z) calcd for C₂₅H₂₂N₂O₂ [M + H]⁺ 383.1760, found 383.1773.

2,4-Bis(benzyloxy)-5-(*m*-tolyl)pyrimidine (22c). White solid, yield 39.02%. ¹H NMR (500 MHz, Chloroform-*d*) δ 8.31 (s, 1H), 7.50 (d, *J* = 7.5 Hz, 2H), 7.41–7.28 (m, 11H), 7.16 (d, *J* = 7.0 Hz, 1H), 5.49 (s, 2H), 5.46 (s, 2H), 2.38 (s, 3H). ¹³C NMR (126 MHz, Chloroform-*d*) δ 167.48, 163.79, 158.04, 138.03, 136.67, 136.32, 133.12, 129.59, 128.49, 128.35, 128.11, 128.04, 127.94, 127.52, 125.92, 116.43, 69.23, 68.32, 21.49. HRMS (ESI, m/z) calcd for C₂₅H₂₃N₂O₂ [M + H]⁺ 383.1760; found 383.1771.

2,4-Bis(benzyloxy)-5-(*p*-tolyl)pyrimidine (22d). White solid, yield 43.70%. ¹H NMR (500 MHz, Chloroform-*d*) δ 8.30 (s, 1H), 7.49 (d, *J* = 7.5 Hz, 2H), 7.44–7.28 (m, 10H), 7.27–7.19 (m, 2H), 5.49 (s, 2H), 5.45 (s, 2H), 2.38 (s, 3H). ¹³C NMR (126 MHz, Chloroform-*d*) δ 167.44, 163.66, 157.90, 137.48, 136.67, 136.30, 129.17, 128.64, 128.48, 128.46, 128.06, 127.57, 116.28, 69.18, 68.31, 21.20. HRMS (ESI, m/z) calcd for C₂₅H₂₃N₂O₂ [M + H]⁺ 383.1760, found 383.1771.

2,4-Bis(benzyloxy)-5-(4-fluorophenyl)pyrimidine (22e). White solid, yield 34.33%. ¹H NMR (500 MHz, Chloroform-*d*) δ 8.28 (s, 1H), 7.49–7.42 (m, 4H), 7.36 (m, 10H), 7.12–7.07 (m, 2H), 5.49 (s, 2H), 5.46 (s, 2H). ¹³C NMR (126 MHz, Chloroform-*d*) δ 167.37, 163.87, 163.35, 161.39, 157.93, 136.57, 136.09, 130.49, 128.55, 128.48, 128.07, 128.06, 127.58, 115.52, 115.44, 115.35, 69.27, 68.45. HRMS (ESI, m/z) calcd for C₂₄H₂₀FN₂O₂ [M + H]⁺ 387.1509, found 387.1519.

2,4-Bis(benzyloxy)-5-(4-chlorophenyl)pyrimidine (22f). White solid, yield 18.47%. ¹H NMR (500 MHz, Chloroform-*d*) δ 8.29 (s, 1H), 7.49 (d, *J* = 7.5 Hz, 2H), 7.45 (d, *J* = 7.5 Hz, 2H), 7.41–7.25 (m, 10H), 5.48 (s, 2H), 5.46 (s, 2H). ¹³C NMR (126 MHz, Chloroform-*d*) δ 167.34, 163.99, 157.98, 136.51, 136.00, 133.66, 131.67, 130.03, 128.65, 128.57, 128.49, 128.10, 128.07, 127.62, 115.23, 69.31, 68.52. HRMS (ESI, m/z) calcd for C₂₄H₂₀ClN₂O₂ [M + H]⁺ 403.1213, found 403.1230.

2,4-Bis(benzyloxy)-5-(2-chlorophenyl)pyrimidine (22g). A colourless liquid, yield 23.55%. ¹H NMR (500 MHz, Chloroform-*d*) δ 8.18 (s, 1H), 7.51–7.46 (m, 2H), 7.46–7.39 (m, 1H), 7.38–7.32 (m, 2H), 7.32–7.19 (m, 9H), 5.45 (s, 2H), 5.43 (s, 2H). ¹³C NMR (126 MHz, Chloroform-*d*) δ 167.82, 164.56, 158.96, 136.64, 136.24, 134.40, 132.59, 131.94, 129.74, 129.55, 128.59, 128.49, 128.25, 128.17, 128.00, 127.68, 114.66, 69.45, 68.46. HRMS (ESI, m/z) calcd for C₂₄H₂₀ClN₂O₂ [M + H]⁺ 403.1213, found 403.1227.

2,4-Bis(benzyloxy)-5-(3-chlorophenyl)pyrimidine (22h). White solid, yield 20.73%. ¹H NMR (500 MHz, Chloroform-*d*) δ 8.31 (s, 1H), 7.54

(s, 1H), 7.52–7.47 (m, 2H), 7.41–7.30 (m, 11H), 5.50 (s, 2H), 5.47 (s, 2H). ^{13}C NMR (126 MHz, Chloroform-*d*) δ 167.36, 164.12, 158.13, 136.49, 135.99, 135.02, 134.29, 129.67, 128.90, 128.57, 128.50, 128.10, 127.71, 127.55, 126.86, 115.08, 69.36, 68.51. HRMS (ESI, *m/z*) calcd for $\text{C}_{24}\text{H}_{20}\text{ClN}_2\text{O}_2$ [$\text{M} + \text{H}$] $^+$ 403.1213, found 403.1226.

2,4-Bis(benzyloxy)-5-(2,4-dichlorophenyl)pyrimidine (22i). White solid, yield 9.56%. ^1H NMR (500 MHz, Chloroform-*d*) δ 8.17 (s, 1H), 7.53–7.47 (m, 3H), 7.41–7.35 (m, 2H), 7.34–7.25 (m, 7H), 7.34–7.25 (m, 7H), 7.21 (d, $J = 8.0$ Hz, 1H), 5.46 (s, 2H), 5.44 (s, 2H). ^{13}C NMR (126 MHz, Chloroform-*d*) δ 167.64, 164.58, 158.86, 136.41, 135.93, 135.08, 134.65, 132.55, 131.08, 129.57, 128.50, 128.45, 128.16, 128.11, 128.03, 127.68, 127.11, 113.49, 69.42, 68.51. HRMS (ESI, *m/z*) calcd for $\text{C}_{24}\text{H}_{19}\text{Cl}_2\text{N}_2\text{O}_2$ [$\text{M} + \text{H}$] $^+$ 437.0824, found 437.0842.

4-(2,4-bis(benzyloxy)pyrimidin-5-yl)phenyl)methanol (22j). White solid, yield 44.04%. ^1H NMR (500 MHz, Chloroform-*d*) δ 8.28 (s, 1H), 7.53–7.47 (m, 4H), 7.43–7.27 (m, 10H), 5.49 (s, 2H), 5.46 (s, 2H), 4.72 (d, $J = 3.5$ Hz, 2H), 1.84 (s, 1H). ^{13}C NMR (126 MHz, DMSO-*d*₆) δ 162.72, 159.08, 153.30, 135.64, 131.86, 131.42, 127.80, 124.21, 123.79, 123.75, 123.28, 122.88, 122.34, 111.27, 64.52, 63.70, 60.29. HRMS (ESI, *m/z*) calcd for $\text{C}_{25}\text{H}_{23}\text{N}_2\text{O}_3$ [$\text{M} + \text{H}$] $^+$ 399.1709, found 399.1722.

4-(2,4-Bis(benzyloxy)pyrimidin-5-yl)phenol (22k). White solid, yield 22.00%. ^1H NMR (500 MHz, DMSO-*d*₆) δ 9.56 (s, 1H), 8.34 (s, 1H), 7.47–7.30 (m, 12H), 6.83–6.78 (m, 2H), 5.46 (s, 2H), 5.41 (s, 2H). ^{13}C NMR (126 MHz, DMSO-*d*₆) δ 166.68, 162.71, 157.36, 156.97, 136.64, 136.25, 129.77, 128.35, 128.33, 127.91, 127.86, 127.82, 127.58, 126.89, 123.09, 115.60, 115.46, 115.14, 68.33, 67.73. HRMS (ESI, *m/z*) calcd for $\text{C}_{24}\text{H}_{21}\text{N}_2\text{O}_3$ [$\text{M} + \text{H}$] $^+$ 385.1552, found 385.1564.

3-(2,4-Bis(benzyloxy)pyrimidin-5-yl)phenol (22l). White solid, yield 18.40%. ^1H NMR (500 MHz, Chloroform-*d*) δ 8.83 (s, 1H), 8.23 (s, 1H), 7.40–7.36 (m, 2H), 7.38–7.10 (m, 9H), 7.08 (s, 1H), 7.00 (d, $J = 7.5$ Hz, 1H), 6.89 (dd, $J = 8.0, 2.5$ Hz, 1H), 5.39 (s, 2H), 5.37 (s, 2H). ^{13}C NMR (126 MHz, Chloroform-*d*) δ 167.58, 163.54, 157.63, 156.90, 136.39, 136.13, 134.14, 129.73, 128.62, 128.59, 128.15, 128.10, 127.86, 127.54, 120.65, 116.39, 116.15, 115.47, 69.48, 68.65. HRMS (ESI, *m/z*) calcd for $\text{C}_{24}\text{H}_{21}\text{N}_2\text{O}_3$ [$\text{M} + \text{H}$] $^+$ 385.1552, found, 385.1562.

2-(2,4-Bis(benzyloxy)pyrimidin-5-yl)phenol (22m). White solid, yield 12.53%. ^1H NMR (500 MHz, Chloroform-*d*) δ 8.30 (s, 1H), 7.52–7.47 (m, 2H), 7.40–7.27 (m, 9H), 7.19 (dd, $J = 7.5, 1.5$ Hz, 1H), 7.05–6.96 (m, 2H), 5.52 (s, 2H), 5.47 (s, 2H). ^{13}C NMR (126 MHz, Chloroform-*d*) δ 166.97, 164.29, 160.23, 153.74, 136.38, 135.48, 131.04, 129.92, 128.66, 128.52, 128.36, 128.13, 128.07, 127.91, 121.19, 120.66, 117.38, 112.81, 69.45, 68.87. HRMS (ESI, *m/z*) calcd for $\text{C}_{24}\text{H}_{20}\text{N}_2\text{O}_3$ [$\text{M} + \text{H}$] $^+$ 385.1552, found 385.1563.

4-(2,4-Bis(benzyloxy)pyrimidin-5-yl)benzoic acid (22n). White solid, yield 20.04%. ^1H NMR (500 MHz, DMSO-*d*₆) δ 12.97 (s, 1H), 8.51 (s, 1H), 7.97 (d, $J = 8.5$ Hz, 2H), 7.72 (d, $J = 8.5$ Hz, 2H), 7.51–7.46 (m, 2H), 7.46–7.29 (m, 8H), 5.49 (s, 2H), 5.46 (s, 2H). ^{13}C NMR (126 MHz, DMSO-*d*₆) δ 166.90, 166.82, 163.60, 158.51, 137.23, 136.44, 135.99, 129.20, 128.70, 128.39, 128.36, 127.98, 127.68, 114.59, 68.59, 68.07. HRMS (ESI, *m/z*) calcd for $\text{C}_{25}\text{H}_{20}\text{N}_2\text{O}_4$ [$\text{M} + \text{H}$] $^+$ 413.1501, found 413.1518.

2,4-Bis(benzyloxy)-5-(thiophen-2-yl)pyrimidine (22o). Brownish solid, yield 15.86%. ^1H NMR (500 MHz, Chloroform-*d*) δ 8.56 (s, 1H),

7.48 (t, $J = 7.0$ Hz, 4H), 7.43–7.30 (m, 8H), 7.09–7.04 (m, 1H), 5.55 (s, 2H), 5.46 (s, 2H). ^{13}C NMR (126 MHz, Chloroform-*d*) δ 166.07, 163.33, 156.38, 136.54, 135.89, 134.48, 128.59, 128.51, 128.22, 128.10, 128.03, 127.30, 125.46, 125.18, 110.61, 69.37, 69.02. HRMS (ESI, *m/z*) calcd for $\text{C}_{22}\text{H}_{19}\text{N}_2\text{O}_2\text{S}$ [$\text{M} + \text{H}$] $^+$ 375.1167, found 375.1181.

2,4-Bis(benzyloxy)-5-(furan-2-yl)pyrimidine (22p). White solid, yield 47.78%. ^1H NMR (500 MHz, Chloroform-*d*) δ 8.75 (s, 1H), 7.51–7.29 (m, 11H), 6.74 (d, $J = 2.5$ Hz, 1H), 6.43 (d, $J = 1.0$ Hz, 1H), 5.54 (s, 2H), 5.46 (s, 2H). ^{13}C NMR (126 MHz, Chloroform-*d*) δ 165.51, 162.97, 154.50, 146.54, 141.70, 136.55, 135.93, 128.69, 128.48, 128.34, 128.12, 128.07, 111.68, 109.53, 107.59, 69.34, 68.99. HRMS (ESI, *m/z*) calcd for $\text{C}_{22}\text{H}_{18}\text{N}_2\text{O}_3$ [$\text{M} + \text{H}$] $^+$ 359.1396, found 359.1409.

Biological evaluation

Cell culture

Three breast cancer cell lines, MCF-7, MDA-MB-231, and 4T1 were used in this study. The cells were purchased from the Institute of Basic Medicine, Chinese Academy of Medical Sciences (Beijing, China). MCF-7 and MDA-MB-23 cells were cultured in DMEM, and 4T1 cells were cultured in RPMI-1640 using 10% foetal bovine serum (FBS) and 1% penicillin-streptomycin solution (PS) in humidified air containing 5% CO_2 at 37 °C.

Antiproliferative activity assay

The antiproliferative activity of the target compounds against the breast cancer cell lines MCF-7, MDA-MB-231, and 4T1 was determined using Cell Counting Kit-8 (Beyotime, Shanghai, China). The target compounds were dissolved in DMSO, diluted with cell culture medium to the desired concentration, and stored at –20 °C before use. Cells were seeded into a 96-well plate at a density of 7000 cells/well (200 μL /well) and incubated overnight. Compound solutions at different concentrations were added and incubated for 48 h. CCK8 solution was added and further incubated for 1–2 h in the dark according to the manufacturer's instructions. Absorbance was measured at a wavelength of 450 nm using Synergy H1 (BioTek Instruments, Inc., Winooski, VT, USA). IC_{50} values were calculated by GraphPad Prism 8 (GraphPad Software, Inc., San Diego, CA, USA). The experiments were performed in triplicate.

Western blotting assay

Primary antibodies against HSP70, HSP90, and GAPDH were purchased from Abcam (Cambridge, MA, USA). Primary antibodies against ERK and AKT were purchased from Beyotime (Shanghai, China). HRP (horseradish peroxidase)-labelled anti-rabbit immunoglobulin G (H + L) secondary antibody was purchased from Abbkine (Redlands, CA, USA). MCF-7 cells were incubated in a 6-well plate at a density of 10^6 cells/well (4 ml/well) at 37 °C for 12 h. The cells were then treated with the compounds and 17-AAG at different concentrations at 37 °C for 24 h. The 6-well plate was placed on ice for 15 min. Cells were collected into a centrifuge tube and lysed by radioimmunoprecipitation (RIPA) lysis solution containing 1% phenylmethanesulphonyl fluoride (PMSF). The lysate was centrifuged at a speed of 14,000 r/min in a cryogenic high-speed centrifuge for 10 min. The cell supernatant was collected to determine the protein content. Cell lysates were mixed with SDS loading buffer and boiled for 20 min. Equal amounts of

protein in cell lysates were separated by 10% sodium dodecyl sulphate–polyacrylamide gel electrophoresis (SDS–PAGE), which was prepared using the PAGE Gel Fast Preparation Kit (Epizyme, PG112, China). The protein on the separating gel was transferred to a polyvinylidene fluoride (PVDF) membrane. The membrane was blocked in skim milk for 80 min and incubated with primary antibody (1:4000) at 4 °C overnight. After further incubation with HRP anti-rabbit IgG (H+L) (1:5000) at room temperature for 1 h, the protein bands were detected with a gel imager (ProteinSimple, San Jose, CA, USA). The density of proteins was determined using AlphaView SA (Alpha Innotech Corp, version 3.4.0.0, San Leandro, CA, USA). The experiments were performed in triplicate.

Fluorescence polarisation (FP) assay

The binding affinity for HSP90 α was evaluated using a commercially available Hsp90 α N-terminal domain assay kit (Catalogue: #50293, BPS Bioscience, CA, USA). According to the manufacturer's instructions, 5x HSP90 assay buffer (5 μ L), 40 mM dithiothreitol (5 μ L), 2 mg/mL BSA (5 μ L), and H₂O (40 μ L) were sequentially added to each well. After the addition of diluted FITC-labelled geldanamycin solution (100 nM, 5 μ L), compounds at different concentrations (10 μ M, 1.0 μ M, 0.1 μ M, 0.01 μ M) were added. The reaction was initiated by the addition of 20 μ L of Hsp90 α (17 ng/ μ L). After 2 h of incubation with slow shaking at room temperature, the fluorescent polarisation was measured using Synergy H1 (BioTek Instruments, Inc.). The excitation and emission wavelengths were 485 nm and 530 nm, respectively. IC₅₀ values were calculated based on the signal changes in the FP competition assay. The experiments were performed in triplicate.

Molecular docking

The crystal structure of the human HSP90 α N-terminus was downloaded from the Protein Data Bank (PDB ID: 1YET)³⁷. Molecular docking was performed using BIOVIA Discovery Studio 2016 (Dassault Systèmes, San Diego, USA). The protein structure was prepared using the "Prepare Protein" procedure before docking. In this procedure, multiple tasks, including building loops, protonation at pH 7.4, and removing water molecules, were performed. Meanwhile, ligands were prepared by the "Prepare Ligand" procedure. The CHARMM force field was used in the preparation of

protein and ligand structures. The binding site was defined using the module "Define site-From PDB Site Records." The coordinates (in XYZ) of the docking region centre were as follows: $x=40.72$, $y=-45.98$, $z=64.47$, and the radius of the active site sphere was 10.3. Docking simulations were performed using CDOCKER, a semiflexible docking program. All other docking parameters were set as default. The protein-ligand docking pose with the highest -CDOCKER_INTERACTION_ENERGY score was taken from the docking results and described.

Statistical analysis

All values obtained from the experiments are expressed as the means \pm SDs. The IC₅₀ values at which the concentration of inhibitor reduces cell viability or enzyme activity by 50% were evaluated by nonlinear regression using GraphPad Prism 8.0 software (GraphPad Software, Inc., La Jolla, USA).

Results and discussions

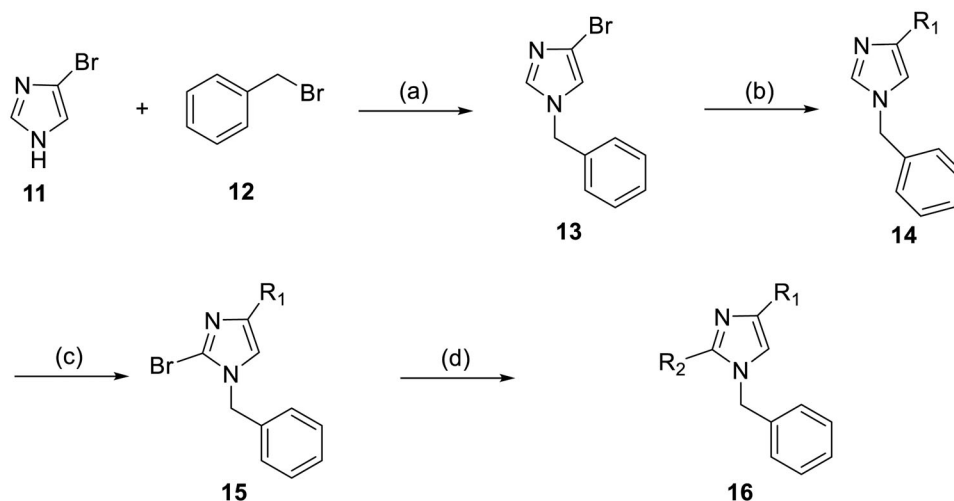
Chemical synthesis

Synthesis of 1-benzyl-2,4-diarylimidazoles 16

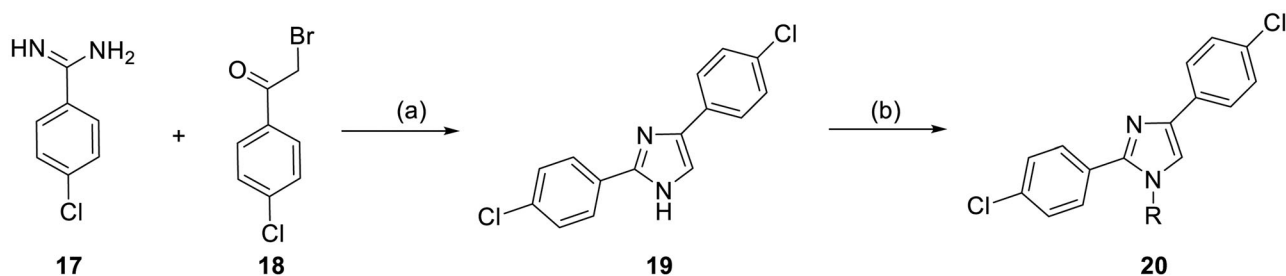
1-Benzyl-2,4-diarylimidazoles **16** were synthesised via a four-step synthetic route (Scheme 1). The benzylation of 4-bromoimidazole **11** with benzyl bromide **12** in the presence of K₂CO₃ provided 1-benzyl-3-bromoimidazole **13**, which further coupled with aryl boronic acid to afford **14** through a Pd(dppf)Cl₂-catalysed Suzuki cross-coupling reaction. The bromination of the imidazole ring of **14** with NBS in CCl₄ gave **15**, which was then converted into the final product **16** through a second Suzuki cross-coupling reaction. The final reaction step always gave low yields, which could be attributed to the debromination of **15**. Simple condition screening experiments revealed that Pd(dppf)Cl₂ was more effective than other palladium catalysts, such as Pd(PPh₃)₄ and Pd(PPh₃)₂Cl₂, at this step.

Synthesis of bis(4-chlorophenyl)imidazoles 20

To further investigate the effect of substituents at the N1 position of the imidazole ring, bis(4-chlorophenyl)imidazoles **20** bearing different functional groups at the N1 position were synthesised (Scheme 2). **19** was prepared by a single-step cyclisation reaction



Scheme 1. Synthetic route for 1-benzyl-2, 4-diarylimidazoles **16**. Reagents and conditions: (a) 4-bromo-1H-imidazole, benzyl bromide, K₂CO₃, acetone, r.t., 22 h; (b) Pd(dppf)Cl₂, Na₂CO₃, 1,4-dioxane/H₂O, N₂, reflux, 4 h; (c) NBS, CCl₄, 35 °C, 14 h; (d) Pd(dppf)Cl₂, Na₂CO₃, 1,4-dioxane/H₂O, N₂, reflux, 4 h.

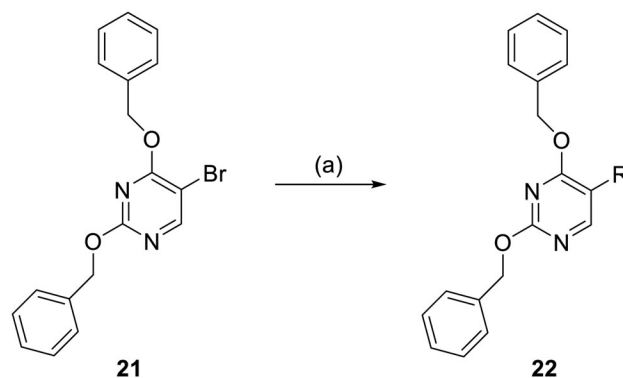


Scheme 2. Synthetic route for 2,4-bis(4-chlorophenyl) imidazoles **20**. Reagents and conditions: (a) NaHCO₃, THF/H₂O, 70 °C, 5 h; (b) alkyl halides, K₂CO₃.

from 4-chlorobenzene-1-carboximidamide hydrochloride **17** and 2-chloro-1-(4-chlorophenyl)ethan-1-one **18** in the presence of NaHCO₃ in THF/H₂O. Treating **19** with different alkyl halides in the presence of K₂CO₃ afforded the *N*-alkylated product **20**.

Synthesis of 2,4-bis(benzyloxy)-5-arylpyrimidines

2,4-Bis(benzyloxy)-5-arylpyrimidines **22** were obtained through a Pd(dppf)Cl₂-catalysed Suzuki cross-coupling reaction between 2,4-bis(benzyloxy)-5-bromopyrimidine **21** and a variety of (hetero)aryl boronic acids in the presence of Na₂CO₃ in 1,4-dioxane/H₂O (Scheme 3).



Scheme 3. Synthetic route for 2,4-bis(benzyloxy)-5-arylpyrimidines **22**. Reagents and conditions: (a) Pd(dppf)Cl₂, Na₂CO₃, 1,4-dioxane/H₂O, N₂, reflux, 4 h.

Biological evaluation

Antiproliferative activity evaluation

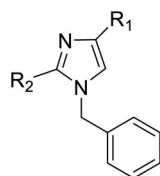
Female breast cancer is the most commonly diagnosed cancer, with an estimated 2.3 million new cases, and the fifth leading cause of cancer mortality, with an estimated 685,000 new deaths around the world in 2020³⁸. HSP90 inhibitors have been extensively studied in clinical trials for the treatment of breast cancer³⁹. Although none has been approved in clinical practice, HSP90 inhibitors have shown great promise in breast cancer therapy. In this study, the antiproliferative activity of the synthesised compounds was evaluated against human breast cancer cell lines MCF-7 and MDA-MB-231 and mouse breast cancer cell line 4T1 using a CCK-8 assay kit. As shown in Table 1, it is remarkable that 1-benzyl-2,4-diphenyl imidazole (**16a**) bearing no substituents on any phenyl ring showed antiproliferative activity against all three cancer cell lines. The effect of substituent R₂ at the C2 position of the imidazole ring was subsequently studied. The methyl group at the *meta*-position of the phenyl ring slightly increased the activity; however, a chlorine atom led to the loss of activity. In the case of the *para*-position, functional groups such as methyl, chloro, and acetyl could preserve the activity, while the hydroxyl group was ineffective. Replacing the phenyl ring with heteroaromatic rings, such as furan and thiophene rings, decreased the activity. The subsequent investigation of substituent R₁ at the C4 position of the imidazole ring revealed that chloro substitution on the phenyl ring was beneficial for increasing activity. Among these 1-benzyl-2,4-diaryl imidazoles, **16j**, **16l**, and **16m** exhibited strong antiproliferative activity with IC₅₀ values in the low micromolar range against three breast cancer cell lines. **8a**, the most potent compound among the imidazolidine-based HSP90 inhibitors, was evaluated for comparison. It exhibited weak antiproliferative activity against MCF-7 and 4T1 cells with IC₅₀ values of 31.25 ± 0.31 μM and 42.10 ± 1.10 μM, respectively, and it was not cytotoxic towards MDA-MB-231 cells. The above results supported our hypothesis that replacing the imidazolidine ring in **8** with a stable aromatic ring could improve the anticancer activity.

The effect of the substituent at the N1 position of the imidazole ring was further studied. The benzyl group proved to be the best substituent at the N1 position. As shown in Table 2, the antiproliferative activity decreased after replacing the benzyl group with other functional groups, such as allyl, aliphatic chain, ester, amide, and aliphatic alcohol. This result indicated that the benzyl group may play essential roles in occupying the space and forming hydrophobic interactions with amino acid residues in the binding site of the HSP90 N-terminus.

In the case of 2,4-bis(benzyloxy)-5-arylpyrimidines **22**, most compounds in this series were ineffective in inhibiting the proliferation of cancer cell lines (Table 3). However, the introduction of the hydroxyl group dramatically increased the activity. Compound **22k**, bearing a 4-hydroxyphenyl group at the C5 position of the pyrimidine ring, exhibited antiproliferative activity with IC₅₀ values of 7.72 ± 0.86, 7.89 ± 0.21, and 7.86 ± 0.76 μM against three breast cancer cell lines. This result suggested that the hydroxyl group may play a crucial role in binding to the target.

Western blotting assay

Treating cells with HSP90 N-terminal inhibitors causes the degradation of HSP90 client proteins and the compensatory expression of heat shock proteins. Protein kinase B (also known as AKT) is a serine/threonine kinase and plays a key role in the PI3K signalling pathway⁴⁰. An extracellular regulated kinase (ERK) is a member of the mitogen-activated protein kinase (MAPK) signalling pathway⁴¹. Both AKT and ERK are client proteins of HSP90 and are essential for cancer progression. The effect of **16l** and **22k** on the expression of the HSP90 client proteins AKT and ERK and the heat shock proteins HSP90 and HSP70 was evaluated by western blotting. As shown in Figure 3, both **16l** and **22k** significantly decreased the expression levels of AKT and ERK in MCF-7 cells, which was consistent with the features of the classical HSP90 N-terminal inhibitor

Table 1. Antiproliferative activity of 1-benzyl-2, 4-diaryl imidazoles **16**.

Comp.	R ₁	R ₂	IC ₅₀ (μM)		
			MCF-7	MDA-MB-231	4T1
16a			19.89 ± 2.76	20.31 ± 2.16	23.40 ± 0.28
16b			14.56 ± 0.25	16.68 ± 0.80	10.54 ± 0.05
16c			>50	>50	>50
16d			15.29 ± 0.65	20.21 ± 0.67	11.69 ± 1.02
16e			14.56 ± 0.92	23.77 ± 0.23	9.87 ± 0.79
16f			14.27 ± 0.43	21.41 ± 0.96	9.48 ± 0.35
16g			>50	>50	>50
16h			>50	>50	>50
16i			>50	29.83 ± 2.06	30.93 ± 3.35
16j			8.13 ± 0.93	14.12 ± 0.11	10.40 ± 0.84
16k			13.95 ± 0.99	14.18 ± 0.86	11.68 ± 0.37
16l			6.16 ± 0.16	7.27 ± 0.16	9.41 ± 0.67

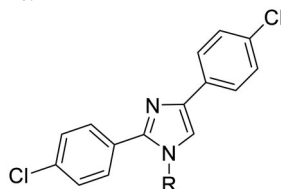
(continued)

Table 1. Continued.

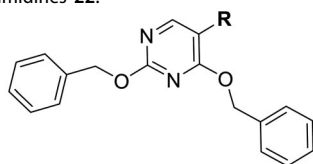
Comp.	R ₁	R ₂	IC ₅₀ (μM)		
			MCF-7	MDA-MB-231	4T1
16m			6.07 ± 0.12	7.80 ± 0.32	10.21 ± 0.80
16n			19.83 ± 0.60	21.20 ± 3.60	10.72 ± 0.99
16o			14.75 ± 0.64	21.15 ± 3.10	22.97 ± 1.70
16p			19.29 ± 0.76	17.24 ± 1.20	22.29 ± 3.20
8a ^[a]	–	–	31.25 ± 0.31	>50	42.10 ± 1.10
17-AAG	–	–	10.60 ± 0.65	39.07 ± 1.30	0.45 ± 0.09

^[a] 8a: 1,3-dibenzyl-2-(5-nitrothiophen-2-yl)imidazolidine.

Table 2. Antiproliferative activity of bis(4-chlorophenyl)imidazoles 20.



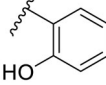
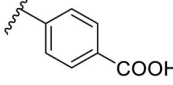
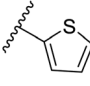
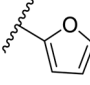
Cmpd.	R	IC ₅₀ (μM)		
		MCF-7	MDA-MB-231	4T1
20a		23.14 ± 3.14	20.79 ± 1.47	22.36 ± 1.99
20b		>50	>50	>50
20c		>50	>50	>50
20d		19.46 ± 2.28	>50	>50
20e		26.67 ± 3.39	39.13 ± 4.38	24.70 ± 3.63
17-AAG	–	10.60 ± 0.65	39.07 ± 1.30	0.45 ± 0.09

Table 3. Antiproliferative activity of 2,4-bis(benzyloxy)-5-arylpyrimidines **22**.

Cmpd.	R	IC ₅₀ (μM)		
		MCF-7	MDA-MB-231	4T1
22a		>50	>50	>50
22b		>50	>50	>50
22c		>50	>50	>50
22d		>50	>50	>50
22e		>50	>50	>50
22f		>50	>50	>50
22g		>50	>50	>50
22h		>50	>50	>50
22i		>50	>50	>50
22j		>50	>50	>50
22k		7.72 ± 0.86	7.89 ± 0.21	7.86 ± 0.76
22l		12.34 ± 0.50	11.17 ± 0.70	8.53 ± 0.50

(continued)

Table 3. Continued.

Cmpd.	R	IC ₅₀ (μM)		
		MCF-7	MDA-MB-231	4T1
22m		13.77 ± 0.28	12.66 ± 0.03	8.25 ± 0.68
22n		28.78 ± 2.09	>50	14.96 ± 2.03
22o		>50	>50	>50
22p		>50	>50	>50
17-AAG		10.60 ± 0.65	39.07 ± 1.30	0.45 ± 0.09

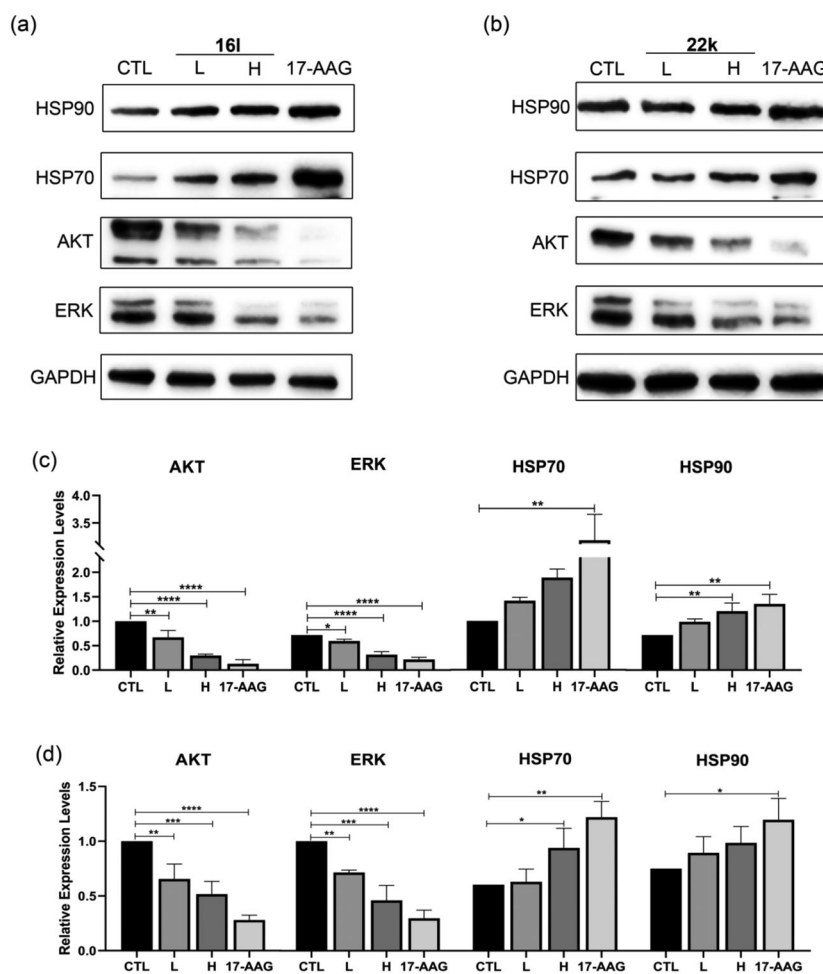


Figure 3. Western blotting assay. (a) (b) Effects of 16l (L: 6 μM; H: 18 μM) and 22k (L: 8 μM; H: 24 μM) on the expression of AKT, ERK, HSP70, and HSP90 in MCF-7 cells, with GAPDH as an internal reference. 17-AAG (15 μM) was used as a positive control. (c) (d) Statistical analysis of western blotting assays of 16l and 22k, respectively. Data are presented as the means ± SDs. **p* < 0.05, ***p* < 0.01, ****p* < 0.001 versus control.

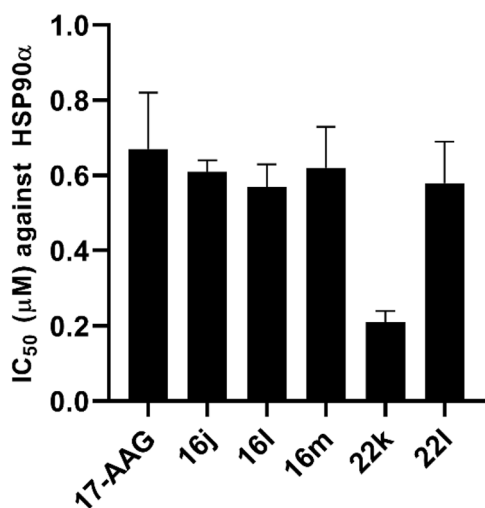


Figure 4. Binding affinity evaluation of representative compounds to HSP90 N-terminus.

17-AAG. It is interesting that, even at a concentration 3 times higher than the IC₅₀ value, the expression level of HSP70 was not significantly increased in the **16l**-treated MCF-7 cells, as was the expression level of HSP90 in the **22k** treated cells. This result suggested that **16l** and **22k** inhibited cancer cell proliferation with a lower level of heat shock response in comparison with 17-AAG.

HSP90 binding affinity evaluation using FP assay

To further verify the binding of the synthesised compounds to the HSP90 N-terminus, the binding affinity of five typical compounds (**16j**, **16l**, **16m**, **22k**, and **22l**) was evaluated using an FP assay. The addition of compounds with HSP90 inhibitory capacity into the assay would compete with the fluorescence probe for binding into HSP90, resulting in a decrease in FP in comparison with the probe alone⁴². As shown in **Figure 4**, all five compounds exhibited similar binding affinities to HP90 in comparison with 17-AAG. Among them, **22k** had the strongest affinity for the HSP90 N-terminus, with an IC₅₀ value of 0.21 ± 0.03 μM.

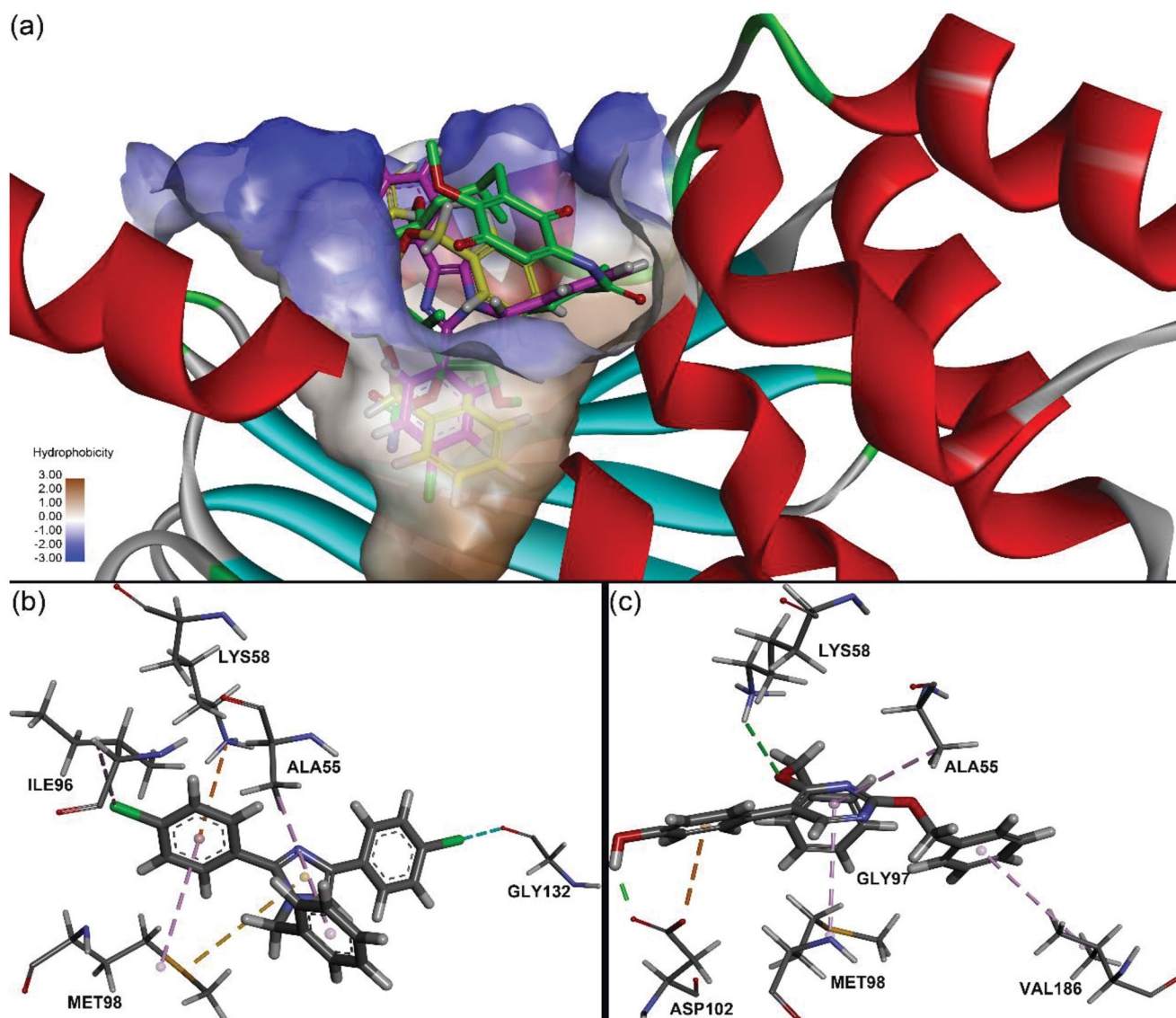


Figure 5. Predicted binding modes of **16l** and **22k** to the N-terminus of HSP90α (PDB code: 1YET). (a) Overlap of **16l** (purple), **22k** (yellow) and geldanamycin (green) in the hydrophobic bond surface of the binding pocket; (b) Interactions between **16l** and HSP90α residues; (c) Interactions between **22k** and HSP90α residues.

Molecular docking study

Molecular docking was performed to predict the binding modes of **16l** and **22k** with the HSP90 α N-terminus. Because the FP assay revealed that **16l** and **22k** could competitively bind to the geldanamycin binding site at the HSP90 α N-terminus, a crystal structure of the HSP90 α N-terminus and geldanamycin (PDB code: 1YET) was used to generate the receptor structure, and the geldanamycin binding site was employed as the active site for docking. To test the feasibility of our docking method, we docked geldanamycin into the prepared HSP90 α N-terminus. The resulting top 10 binding poses were very similar to the experimental pose, with all RMSD values less than 1 Å, which suggested that our docking procedure could afford good pose reproduction (Figure S115 in the supporting information). The top-scoring pose has a -CDOCKER_INTERACTION_ENERGY score of 65.32 with an RMSD value of 0.70. As shown in Figure 5(a), **16l** and **22k** were successfully docked into the binding pocket of geldanamycin at the N-terminus of HSP90 α with -CDOCKER_INTERACTION_ENERGY scores of 36.36 and 55.08, respectively.

16l presented a "T-shaped lock" conformation and was possibly able to block the entrance of ATP into the binding pocket. The benzyloxy group at the N1 position of **16l** was directed towards the bottom of the binding pocket, while two 4-chlorophenyl groups were positioned at the mouth of the binding pocket. **16l** may form a halogen bond with GLY132, a Pi-cation interaction with LYS58, a Pi-sulphur interaction with MET98, and multiple hydrophobic interactions with residues ALA55, ILE96, and MET98 (Figure 5b). In the case of **22k**, the benzyloxy group at the C2 position of the pyrimidine ring was oriented towards the bottom of the binding pocket. It should be noted that **22k** may have formed hydrogen bonds with LYS58 and ASP102 (Figure 5c). The hydrogen bond interaction between the hydroxyl group of **22k** and ASP102 indicated that the hydroxyl group may be important for stabilising the protein-ligand complex. This result is consistent with the observations in the biological evaluation that the introduction of the hydroxyl group enhanced the antiproliferative activity. In addition, hydrophobic interactions with residues ALA55, MET98, and VAL186 and a Pi-Anion interaction with ASP102 were observed in the predicted binding mode of **22k** and the HSP90 N-terminus.

Conclusion

In summary, our work discovered two kinds of novel HSP90 N-terminal inhibitors bearing 2,4-diarylimidazole and 2,4-bis(benzyloxy)-5-arylpyrimidine as their scaffolds. **16l** and **22k** exhibited strong antiproliferative activities against three breast cancer cell lines, MCF-7, MDA-MB-231, and 4T1. Their inhibitory activity towards the HSP90 N-terminus was validated by western blotting and FP assays, and possible interaction modes were predicted by molecular docking. **16l** and **22k** can serve as a starting point for more in-depth research on anticancer drugs targeting the HSP90 N-terminus. Our future efforts will focus on evaluating the anticancer activity *in vivo* and investigating the pharmacokinetic behaviours of **16l** and **22k**.

Disclosure statement

The authors report no conflicts of interest.

Funding

This work is funded by the Natural Science Foundation of Liaoning Province of China [Grant No. 2020-MS-105], and the

Fundamental Research Funds for the Central Universities [Grant No. DUT20LK20; DUT22YG111].

ORCID

Yajun Liu  <http://orcid.org/0000-0002-9539-7279>

References

- Freilich R, Arhar T, Abrams JL, Gestwicki JE. Protein-protein interactions in the molecular chaperone network. *Acc Chem Res.* 2018;51(4):940–949.
- Kim YE, Hipp MS, Bracher A, Hayer-Hartl M, Hartl FU. Molecular chaperone functions in protein folding and proteostasis. *Annu Rev Biochem.* 2013;82:323–355.
- Hoter A, El-Sabban ME, Naim HY. The HSP90 family: structure, regulation, function, and implications in health and disease. *IJMS.* 2018;19(9):2560.
- Schopf FH, Biebl MM, Buchner J. The HSP90 chaperone machinery. *Nat Rev Mol Cell Biol.* 2017;18(6):345–360.
- Picard D. Heat-shock protein 90, a chaperone for folding and regulation. *Cell Mol Life Sci.* 2002;59(10):1640–1648.
- Whitesell L, Lindquist SL. HSP90 and the chaperoning of cancer. *Nat Rev Cancer.* 2005;5(10):761–772.
- Kamal A, Thao L, Sensintaffar J, Zhang L, Boehm MF, Fritz LC, Burrows FJ. A high-affinity conformation of Hsp90 confers tumour selectivity on Hsp90 inhibitors. *Nature.* 2003;425(6956):407–410.
- Miyata Y, Nakamoto H, Neckers L. The therapeutic target Hsp90 and cancer hallmarks. *Curr Pharm Des.* 2013;19(3):347–365.
- Serwetnyk MA, Blagg BSJ. The disruption of protein-protein interactions with co-chaperones and client substrates as a strategy towards Hsp90 inhibition. *Acta Pharm Sin B.* 2021;11(6):1446–1468.
- Trepel J, Mollapour M, Giaccone G, Neckers L. Targeting the dynamic HSP90 complex in cancer. *Nat Rev Cancer.* 2010;10(8):537–549.
- Bohush A, Bieganski P, Filipek A. Hsp90 and its co-chaperones in neurodegenerative diseases. *IJMS.* 2019;20(20):4976.
- Fuhrmann-Stroissnigg H, Ling YY, Zhao J, McGowan SJ, Zhu Y, Brooks RW, Grassi D, Gregg SQ, Stripay JL, Dorronsoro A, et al. Identification of HSP90 inhibitors as a novel class of senolytics. *Nat Commun.* 2017;8(1):422.
- Huang DS, LeBlanc EV, Shekhar-Guturja T, Robbins N, Krysan DJ, Pizarro J, Whitesell L, Cowen LE, Brown LE. Design and synthesis of fungal-selective resorcyate aminopyrazole Hsp90 inhibitors. *J Med Chem.* 2020;63(5):2139–2180.
- Lubkowska A, Pluta W, Strońska A, Lalko A. Role of heat shock proteins (HSP70 and HSP90) in viral infection. *IJMS.* 2021;22(17):9366.
- Noddings CM, Wang RY-R, Johnson JL, Agard DA. Structure of Hsp90-p23-GR reveals the Hsp90 client-remodelling mechanism. *Nature.* 2022;601(7893):465–469.
- Verba KA, Wang RY-R, Arakawa A, Liu Y, Shirouzu M, Yokoyama S, Agard DA. Atomic structure of Hsp90-Cdc37-Cdk4 reveals that Hsp90 traps and stabilizes an unfolded kinase. *Science.* 2016;352(6293):1542–1547.
- Li L, Chen N-N, You Q-D, Xu X-L. An updated patent review of anticancer Hsp90 inhibitors (2013-present). *Expert Opin Ther Pat.* 2021;31(1):67–80.

18. Xiao Y, Liu Y. Recent advances in the discovery of novel HSP90 inhibitors: an update from 2014. *Curr Drug Targets*. 2020;21(3):302–317.
19. Bickel D, Gohlke H. C-terminal modulators of heat shock protein of 90 kDa (HSP90): state of development and modes of action. *Bioorg Med Chem*. 2019;27(21):115080.
20. Wang Y, Mcalpine SR. N-terminal and C-terminal modulation of Hsp90 produce dissimilar phenotypes. *Chem Commun*. 2015;51(8):1410–1413.
21. Li L, Wang L, You Q-D, Xu X-L. Heat shock protein 90 inhibitors: an update on achievements, challenges, and future directions. *J Med Chem*. 2020;63(5):1798–1822.
22. Azimi A, Caramuta S, Seashore-Ludlow B, Boström J, Robinson JL, Edfors F, Tuominen R, Kemper K, Krijgsman O, Peeper DS, et al. Targeting CDK2 overcomes melanoma resistance against BRAF and Hsp90 inhibitors. *Mol Syst Biol*. 2018;14(3):e7858.
23. Eroglu Z, Chen YA, Gibney GT, Weber JS, Kudchadkar RR, Khushalani NI, Markowitz J, Brohl AS, Tetteh LF, Ramadan H, et al. Combined BRAF and HSP90 inhibition in patients with unresectable BRAF (V600E)-mutant melanoma. *Clin Cancer Res*. 2018;24(22):5516–5524.
24. Birbo B, Madu EE, Madu CO, Jain A, Lu Y. Role of HSP90 in cancer. *IJMS*. 2021;22(19):10317.
25. Solárová Z, Mojžiš J, Solár P. Hsp90 inhibitor as a sensitizer of cancer cells to different therapies (review). *Int J Oncol*. 2015; 46(3):907–926.
26. Mortensen ACL, Mohajershojai T, Hariri M, Pettersson M, Spiegelberg D. Overcoming limitations of cisplatin therapy by additional treatment with the HSP90 inhibitor onalespib. *Front Oncol*. 2020;10(532285):532285.
27. Liu Y, Liu X, Li L, Dai R, Shi M, Xue H, Liu Y, Wang H. Identification and structure-activity studies of 1,3-Dibenzyl-2-aryl imidazolidines as novel Hsp90 inhibitors. *Molecules*. 2019;24(11):2105.
28. Hwang JY, Kim H-Y, Jo S, Park E, Choi J, Kong S, Park D-S, Heo JM, Lee JS, Ko Y, et al. Synthesis and evaluation of hexahydropyrimidines and diamines as novel hepatitis C virus inhibitors. *Eur J Med Chem*. 2013;70:315–325.
29. Godin G, Levrand B, Trachsel A, Lehn J-M, Herrmann A. Reversible formation of amins: a new strategy to control the release of bioactive volatiles from dynamic mixtures. *Chem Commun*. 2010;46(18):3125–3127.
30. Buchs Née Levrand B, Godin G, Trachsel A, de Saint Laumer J-Y, Lehn J-M, Herrmann A. Reversible amination: controlling the evaporation of bioactive volatiles by dynamic combinatorial/covalent chemistry. *Eur J Org Chem*. 2011; 2011(4):681–695.
31. Zhang L, Peng X-M, Damu GLV, Geng R-X, Zhou C-H. Comprehensive review in current developments of imidazole-based medicinal chemistry. *Med Res Rev*. 2014;34(2): 340–437.
32. Jeelan BN, Goudgaon NM. A comprehensive review on pyrimidine analogs-versatile scaffold with medicinal and biological potential. *J Mol Struct*. 2021;1246:131168.
33. Senecal TD, Shu W, Buchwald SL. A general, practical palladium-catalyzed cyanation of (hetero)aryl chlorides and bromides. *Angew Chem Int Ed Engl*. 2013;52(38):10035–10039.
34. Wang D, Haseltine J. A comparison of phenylboronic acid and phenyltrimethyltin in the palladium-catalyzed arylation of 1,5-dialkylimidazoles. *J Heter Chem*. 1994;31(6): 1637–1639.
35. O'Connell JF, Parquette J, Yelle WE, Wang W, Rapoport H. Convenient synthesis of methyl 1-methyl-2,4-dibromo-5-imidazolecarboxylate. *Synthesis*. 1988;1988(10):767–771.
36. Li B, Chiu CK-F, Hank RF, Murry J, Roth J, Tobiassen H. An optimized process for formation of 2,4-disubstituted imidazoles from condensation of amidines and α -haloketones. *Org Process Res Dev*. 2002;6(5):682–683. —
37. Stebbins CE, Russo AA, Schneider C, Rosen N, Hartl FU, Pavletich NP. Crystal structure of an Hsp90-geldanamycin complex: targeting of a protein chaperone by an antitumor agent. *Cell*. 1997;89(2):239–250.
38. Sung H, Ferlay J, Siegel RL, Laversanne M, Soerjomataram I, Jemal A, Bray F. Global cancer statistics 2020: GLOBOCAN estimates of incidence and mortality worldwide for 36 cancers in 185 countries. *CA A Cancer J Clin*. 2021;71(3): 209–249.
39. Zagouri F, Sergentanis TN, Chrysikos D, Papadimitriou CA, Dimopoulos M-A, Psaltopoulou T. Hsp90 inhibitors in breast cancer: a systematic review. *Breast*. 2013;22(5):569–578.
40. Song M, Bode AM, Dong Z, Lee M-H. AKT as a therapeutic target for cancer. *Cancer Res*. 2019;79(6):1019–1031.
41. Liu F, Yang X, Geng M, Huang M. Targeting ERK, an Achilles' Heel of the MAPK pathway, in cancer therapy. *Acta Pharm Sin B*. 2018;8(4):552–562.
42. Howes R, Barril X, Dymock BW, Grant K, Northfield CJ, Robertson AGS, Surgenor A, Wayne J, Wright L, James K, et al. A fluorescence polarization assay for inhibitors of Hsp90. *Anal Biochem*. 2006;350(2):202–213.